Differentiating bulk nanobubbles from nanodroplets and nanoparticles

Available online at www.sciencedirect.com

ScienceDirect

Current Opinion in
Colloid & Interface Science

Differentiating bulk nanobubbles from nanodroplets and nanoparticles

Fredrik Eklund[1], Muidh Alheshibri[2,3] and Jan Swenson[1]

Abstract

History has shown that it is not as easy as one might think to differentiate between bulk nanobubbles and nanodroplets or nanoparticles. It is generally easy to detect colloids (i.e. something that looks different, e.g. scatters light differently than its surrounding solvent), but less easy to determine the nature of these colloids. This has led to misinterpretations in the literature, where nanodroplets or nanoparticles have mistakenly been assumed to be nanobubbles. In this paper, we review a multitude of experimental methods and approaches to prove the existence of bulk nanobubbles. We conclude that combinations of optical detection with physical perturbations such as pressure or ultrasound, or phase-sensitive holographic methods are the most promising and convenient approaches.

Addresses

[1] Division of Nano and Biophysics, Department of Physics, Chalmers University of Technology, SE-41296 Göteborg, Sweden
[2] Department of Basic Sciences, Deanship of Preparatory Year and Supporting Studies, Imam Abdulrahman Bin Faisal University, P.O. Box 1982, Dammam 31441, Saudi Arabia
[3] Basic & Applied Scientific Research Center, Imam Abdulrahman Bin Faisal University, P.O. Box 1982, Dammam 31441, Saudi Arabia

Corresponding author: Eklund, Fredrik (fredrik@eklund.com)

Current Opinion in Colloid & Interface Science 2021, **53**:101427

This review comes from a themed issue on **Hot Topic: Nanobubbles & Nanodroplets**

Edited by **Vince Craig**, **Marie Pierre Krafft** and **Thomas Zemb**

For a complete overview see the Issue and the Editorial

https://doi.org/10.1016/j.cocis.2021.101427

Keywords

Nanobubbles, Microbubbles, Ultrafine bubbles, Colloidal dispersions, Nanoparticle tracking analysis, Dynamic light scattering, Digital holographic microscopy.

Introduction

In recent years, nanobubbles and small microbubbles have been explored and used in many technical and medical applications [1]. In medicine, bubbles in the size (diameter) range 0.5–10 μm are used as contrast agents in ultrasound imaging, and are increasingly explored for therapeutic purposes [2,3]. In this context, bubbles smaller than 1 μm are being researched because of their ability to better penetrate biological tissue. In the medical field, micro- and nanobubbles are stabilized by a well-defined coating of surface-active molecules or particles [2], whereas in industrial/technical applications, nanobubbles are generally generated in natural water or aqueous solutions without addition of any specific bubble-stabilizing surfactants. In this review, we will use the term nanobubbles for bubbles with a diameter less than 1 μm. Despite that 'nano' has been recommended to be used only for entities smaller than 100 nm, this is the commonly used nomenclature in the field. Other terms for this size range are 'ultrafine bubbles' (recommended by the international standardization organization, ISO) and 'submicron bubbles.'

Generation of nanobubbles has been explored in many technical applications, such as agriculture [4], aquaculture [5], cleaning [6], environmental remediation [7,8], flotation, and water treatment [9]. Many promising technical results have been achieved, which have been attributed to long-lived nanobubbles, which remain in the water for hours and days. However, the nature of the generated nanobubbles remains unknown, both in terms of their stabilization mechanism and their composition. It has even been questioned if long-lived light scattering submicron entities detected after vigorous generation of visible microbubbles really are nanobubbles in every case, and not particle agglomerates or oil droplets [10–15] (F Eklund, PhD Thesis, Chalmers UoT, 2020). Perhaps the technical results achieved with various nanobubble generators are due to increased concentration of dissolved oxygen (agriculture, aquaculture), generation of reactive oxygen species (agriculture, aquaculture), nucleation of surface nanobubbles on suspended particles (flotation), and short-lived micro- and nanobubbles with a lifetime of seconds or perhaps a few minutes? It is obvious that there is a strong need for analytical methods, which can differentiate nanobubbles from oil droplets and particles in industrial applications. A need for analytical methods being able to differentiate between nanobubbles and other colloids is also evident in the medical field, where nanobubble preparations are generally heterodisperse mixtures of bubbles, liposomes, and solid particles, which are not always easy to differentiate. The aim of this review is therefore to discuss advantages and disadvantages of

commonly used methods to do this. However, first the physical properties of nanobubbles will be discussed to understand their behaviors and how they are affected by different treatments.

Based on diffusion analysis, an uncoated bubble with a diameter less than 1 μm is expected to have a lifetime of a few milliseconds or less [16]. The primary driving force for dissolution of such small bubbles is the Laplace pressure, which arises because of the surface tension of a curved surface. As seen in Figure 1, the internal excess pressure of a nanobubble is considerable and it is enough to drive the bubble to rapid dissolution even in water with more than 50% oversaturation of dissolved gas.

Any explanation for nanobubbles with a life-time on the magnitude of minutes or more need to relate to the Laplace pressure. In the case of coated nanobubbles, the coating serves to decrease the surface tension down to extremely low values and thus remove the Laplace pressure more or less entirely [18]. Several other stability mechanisms have been suggested and these may predict bubbles with somewhat different properties. For instance, the dynamic equilibrium model predicts nanobubbles with a substantial amount of adsorbed hydrophobic material [19]. The adsorbed material could give such bubbles a different refractive index (RI) and thus different optical properties compared to a clean bubble or a bubble with a thin surfactant coating. Furthermore, the model predicts nanobubbles with an intact Laplace pressure, which means they will contain up to more than 10 times as much gas as bubbles without any Laplace pressure. A third type of mechanism stresses the surface charge as a source of stability [20,21] and thus predicts a high magnitude of zeta potential and a stability dependence on this property. This would mean that the bubble stability will depend on pH and ionic strength of the solution, but adsorbed material will not be necessary.

Figure 1

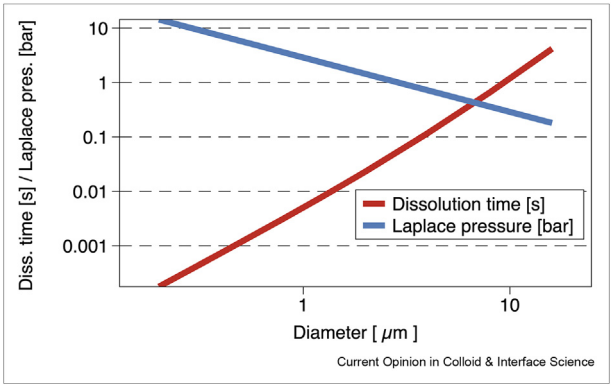

Laplace pressure and dissolution time. Red line: Time for complete dissolution of an air bubble with a surface tension of 72 mN/m, in water with 100% air saturation, and at 293 K. Calculated from eq (17) in Ref. [17]. Blue line: Laplace pressure under the same conditions. Both axes are logarithmic.

At a typical nanobubble concentration of 10^8/cm^3, 0.1 μm diameter bubbles make out only a volume fraction of 10^{-7} relative to the liquid volume. For 1 μm bubbles, the volume fraction is 10^{-4}, which is higher but still rather low. If such bubbles have no Laplace pressure, the gas in them amount to 0.0001 mg/l (0.1 μm) or 0.1 mg/l (1 μm), which is very little in relation to the equilibrium concentration of dissolved nitrogen (19 mg/l) and oxygen (4.3 mg/l) at 20 °C. If the air–water interface has its usual surface tension of 72 mN/m, the smaller bubble will have an order of magnitude higher internal pressure and thus gas content. From an analytical perspective, optical light scattering methods can readily detect nanobubbles in this size and concentration range, but for methods devised to detect the gas inside the bubbles (see section Gas detection), the low volume and mass fraction comprises a considerable challenge.

Water and aqueous solutions normally contain gas bubbles, both free floating bulk bubbles and bubbles on surfaces and on the surface of dispersed particles. Such 'gaseous nuclei' are required for heterogeneous nucleation of macroscopic bubbles in boiling and cavitation under normal conditions [22,23]. In water free of gaseous nuclei, the boiling temperature as well as the subpressure required for cavitation is considerably elevated. However, the concentration of such 'cavitation nuclei' is low. For nuclei with a low enough curvature to be susceptible to mild subpressures of a few bar, typical for hydrodynamic cavitation, the bulk concentration is typically less than 1/cm^3 [24,25]. These nuclei are therefore difficult to characterize and are detected indirectly by the macroscopic cavitation bubbles they give rise to. In contrast, bubble concentrations typically reported in medical and industrial applications are in the range of 10^6–10^{10}/cm^3. Such concentrations can be detected by common optical methods such as nanoparticle tracking analysis (NTA) and dynamic light scattering (DLS). Much lower concentrations are, however, difficult to detect and characterize. This review will focus on methods for detection and characterization of bubbles with a concentration $>10^6$/cm^3. It will furthermore focus primarily on nanobubbles with a lifetime of several minutes or more, whereas short-lived bubbles will be only briefly considered.

Optical methods

Light scattering methods are fundamental in nanobubble studies as well as for detecting and characterizing colloidal particles in general. The emergence of powerful and user-friendly equipment for DLS can be said to have given birth to, or at least strongly boosted, the nanobubble field. Later NTA became popular,

providing more detailed size distribution data. A simple light scattering method, often used in practical settings to detect (assumed) nanobubbles, is to visually examine the light scattered when illuminating a water sample with a common laser pointer. However, light scattering methods can generally not see a difference between gaseous bubbles and solid particles or droplets. Therefore, optical methods based on phase contrast are needed to determine whether the RI is higher (as in the case of most solid particles and liquid droplets) or lower (as for gaseous bubbles) than for water. In the last part of this section, we describe such methods.

DLS

In DLS, a laser beam illuminates a liquid sample in a cuvette of typically around 10 mm width. Light scattered by particles in the sample is detected by a detector located at a certain angle relative to the illumination beam. Depending on the size of the dispersed particles, the detected signal will fluctuate faster or slower due to the Brownian motion of the particles. The method is very sensitive and can detect particles in a wide size range, from less than a nanometer [26] to several micrometers. It does, however, analyze all the illuminated particles as an ensemble, and although there are algorithms to analyze polydisperse samples, the ability of the method to resolve a heterogeneous particle size distribution as well as different types of particles is limited [27].

NTA

In NTA, the liquid sample is viewed in a regular microscope while illuminated at about 90° angle to the line of view. Dispersed particles are viewed and video recorded as bright dots against a black background. The Brownian movement of individual particles is analyzed to determine their hydrodynamic size. The lower detection limit is about 30–40 nm depending on the RI difference between particle and liquid. As nanoparticles are tracked individually, a more detailed size distribution can be determined than with DLS. To cover the whole submicron size range, it is, however, necessary to make several recordings with different optical settings. Owing to the stochastic nature of Brownian motion, the determined size will often have a considerable spread and the results are therefore still somewhat statistical. The method is generally sensitive to settings for recording and analysis [28]. By quantifying the scattered intensity from each particle, it is in principle possible to use the method to determine the RI difference between particles and the surrounding medium [29]. However, in practice, this is difficult due to nonuniform illumination and varying scattering intensity as the particles drift in and out of focus [30]. It is in any case not possible to differentiate between positive and negative RI difference to identify nanobubbles.

Optical flow cytometry

In optical flow cytometry, a narrow hydrodynamically focused flow of liquid is passing an optical detector at high speed, while illuminated by a laser. A detector placed at a certain angle to the illuminating beam counts the particles one by one by their scattered light. The essential purpose is to quantify the number of particles and it is traditionally used to count cells (cyto = cell). It is thus a common instrument in life science laboratories and has perhaps for that reason been used to characterize contrast agent bubbles [31,32], but not industrial nanobubbles. One advantage is the very high throughput, although the high speed also limits the amount of information collected for each particle. By using two or more detectors at different scattering angles, it is possible to identify different populations in the same sample based on their different morphology or RI. Like other light scattering methods, it cannot differentiate between a positive and a negative RI difference between particle and medium. Common flow cytometers have a lower detection limit of 0.3 μm diameter [33] or higher, although it is technically possible to reach lower.

Holography and phase-contrast microscopy

Light that is transmitted through a liquid sample will carry phase information, which is not available from scattered light alone. Light passing a solid particle will slow down and achieve a phase shift compared with light not passing the particle. For a gaseous bubble, the phase shift will be of opposite sign and by measuring the phase shift, it is thus possible to differentiate gaseous bubbles from solid particles and droplets. Except for some fluorinated hydrocarbons, it is under normal circumstances only gas bubbles (RI = 1.00) that have an RI lower than water (RI = 1.33). Analog phase contrast microscopy [34] is a well-established technique to study biological specimens, which has also been applied to nano- and microbubbles immobilized in gel [35]. It is, however, a qualitative rather than quantitative method and usually applied to immobile samples. There is, however, a multitude of digital holographic microscopy (DHM) methods that can quantify the RI of individual particles and these are therefore very useful for the detection of bubbles. Digital holographic imaging of nanobubbles was first reported by Bunkin [36], but was restricted to slowly diffusing bubbles close to the cover glass because of long exposure time, and also restricted to manual detection and characterization of each bubble. Using inline holography, automated characterization of particles down to 0.5 μm diameter has been demonstrated [37]. This technique has also been used to detect microbubbles [38]. Off-axis DHM, using a separate reference beam, is more complicated and computationally heavy, but has recently been showing promising results. Midtvedt, Eklund et al. demonstrated tracking and characterization of surfactant-stabilized nanobubbles as small as 0.3 μm and differentiated

them from solid particles in the same dispersion [39] (Figure 2b,c). Further improvements have allowed a lower detection limit to be reached and for strong light scatterers, such as bubbles and polystyrene particles, the smallest detectable size is presently 0.15 μm (unpublished data). The method allows detection and separate characterization of different particle populations in the same dispersion, even if they are close in size and RI (Figure 2a). Furthermore, in addition to hydrodynamic size, an optical size can also be determined [40], using only a few image frames and thus allowing monitoring of short-term changes in optical properties of a particle, droplet, or bubble.

Response of bubbles to physical perturbations

Although light scattering methods cannot differentiate bubbles from particles and droplets, they can be used in combination with various physical methods to detect bubbles. This can be done by comparing light scattering data before and after subjecting the bubble dispersion to pressure, vacuum/undersaturation, centrifugation, or other perturbations. This approach requires that a substantial fraction of the light scattering detections are bubbles, if only a few percent of the detections are bubbles, changes in light scattering will not be significant. Most preferable is to collect light scattering data while simultaneously exposing the sample to said physical perturbations, as this will provide more information and probe shorter time scales. Monitoring individual particles rather than the entire ensemble also makes it possible to detect a smaller bubble fraction in a heterogeneous dispersion. In addition to pressure, vacuum/undersaturation, and centrifugation treated in this section, also ultrasound resonance is a perturbation, which is useful to combine with optical detection, ultrasound is treated in section Ultrasound response and cavitation.

Pressure

The response of bubbles to application of external pressure is very different from that of droplets and solid particles, because of the high compressibility of gas, as well as the pressure sensitivity of the equilibrium between gas and liquid as expressed by Henry's law. Removal of very small concentrations of naturally occurring gaseous nuclei by pressurization is well known to affect water's susceptibility to cavitation [41]. Destruction of optically detected micro- and nanobubbles has been reported in several cases [39,42,43]. There are several possible mechanisms by which pressure may destroy bubbles, presumably cavitation and bubble growth at pressure release is the most important. Not only the pressure magnitude, but also the rate of pressure release [44] may thus be important. The parameters used vary greatly between different reports, and also the sensitivity of the investigated bubbles. To complicate matters, depressurization has also been reported to generate nanobubbles, on dispersed particles as well as in bulk, rather than destroy them [45–47]. Bubbles stabilized by unknown adsorbed material in sea water [43] were sensitive to comparably small pressure changes compared with coated bubbles in a commercial contrast agent [48]. There is a certain possibility that droplets of oil, which is slightly water soluble and/or volatile, could respond to pressure changes as well, which could lead to false bubble detections when only making optical measurement before and after

Figure 2

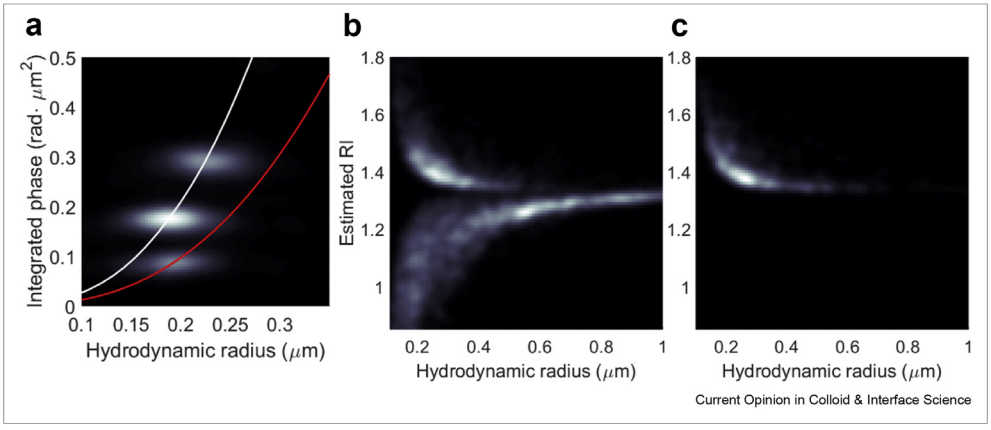

Holographic NTA using off-axis configuration. **(a)** Three different particle populations close in size and RI in the same dispersion are readily identified. The white line corresponds to particles with RI = 1.58 (polystyrene) and the red line to RI = 1.45 (silica). **(b)** Dispersion of nanobubbles stabilized by sorbitan-based surfactants. Solid particles of insoluble surfactant have RI > 1.33 and bubbles have RI < 1.33. The larger bubbles are clusters of individual bubbles with an effective RI closer to water than individual bubbles. The large spread in RI for small bubbles is due to it being calculated from the hydrodynamic size, which in turn has a large spread because of the stochastic nature of Brownian motion. **(c)** Following a pressure treatment at 20 bar, the bubbles disappeared. Reprinted from Midtvedt, D.; Eklund, F.; Olsén, E.; Midtvedt, B.; Swenson, J.; Höök, F., Size and Refractive Index Determination of Subwavelength Particles and Air Bubbles by Holographic Nanoparticle Tracking Analysis. Anal. Chem. 2020, 92 (2).

pressurization. A better way is, therefore, to monitor the bubbles optically during the entire pressure cycle, during which bubbles will contract and subsequently expand again, thereby clearly demonstrating their compressibility. Monitoring of bubble compression by optical microscopy has been reported for bubbles in sea water [43] and distilled water/gel [35]. Monitoring of bubble compression during DLS measurement was recently demonstrated by Alheshibri et al. for contrast agent bubbles [48]. This method was also used to determine that suspected nanobubbles produced by ethanol–water mixing [10], commercial nanobubble generators [11], and by a chemical reaction [49] were not actually bubbles. Pressurization combined with optical methods is one of the more useful approaches to nanobubble detection, but there is room for further investigations on pressurization parameters and how they may influence formation and destruction of bubbles of different types, as well as if oil droplets can potentially respond to pressurization under certain conditions.

Vacuum/undersaturation

Beside the mechanical effect of depressurization covered in the previous subsection, vacuum can be used to decrease the concentration of dissolved gas in water and thereby dissolve nanobubbles. As it takes a long time for gas molecules to diffuse through water, a long time under vacuum and/or stirring or a very small sample size is needed. Vacuum treatments combined with optical methods have been used to prove [14,50] or disprove [13,14] nanobubbles in several cases. An alternative, faster method is to mix the nanobubble sample with previously degassed water to dissolve any bubbles [39,51]. A disadvantage of these approaches is that volatile oil droplets may transition to large gas bubbles, which subsequently float and disappear from the solution, causing distorted results. In fact, phase change of oil droplets to gas bubbles caused by ultrasound has previously been practically demonstrated for ultrasound contrast [3]. Another aspect is that different types of nanobubbles may have different resistance to gas undersaturation. Some types of coated micro- and nanobubbles may have considerably extended lifetimes in slightly undersaturated solutions [52,53]. For uncoated nanobubbles, several stability mechanisms have been suggested, of which the dynamic equilibrium model predicts a certain stability against gas undersaturation [19].

Another approach that has been used in several cases [54–56] is to degas the solution before nanobubble generation. If no light scattering entities appear after bubble generation in degassed water, it is concluded that the light scatterers appearing in the other case are nanobubbles. However, vigorous generation of short-lived microbubbles may collect and agglomerate nanoparticles or oil on their surface, which remain in dispersion after the bubbles have dissolved. In addition, volatile oils may be removed by the vacuum, which could prevent the subsequent formation of nanodroplets, which could be mistaken for bubbles. Any effects of degassing before nanobubble generation must therefore be considered as rather weak evidence of nanobubbles.

Dissolution of nanobubbles in undersaturated water is a useful method, but the results may differ between different bubble types and oil droplets may still be mistaken for nanobubbles. There is room for more research on how different degrees of undersaturation affect different bubble types as well as volatile oil droplets.

Centrifugation

Centrifugation can separate buoyant colloids such as bubbles or oil droplets from sedimenting colloids such as solid particles, and also separate different size fractions of colloids. Centrifugation has been commonly used in the medical field to separate coated bubbles of different size fractions [57,58]. It has also been used in other nanobubble research: Rak et al. [12] centrifugated dispersions at incrementally higher centrifugation speed and made DLS measurements directly on the centrifugation tube after each increment. By using two different sample volumes in the tubes, positively and negatively buoyant colloids could be differentiated. This is due to the fact that sedimenting particles had different pathlength to travel in the two cases and thus gave different results, whereas buoyant particles had the same pathlength to travel and thus gave the same result between the two experiments. Furthermore, combining the measured size and sedimentation rate, the density of the colloids could be estimated. This was used to show that light scattering particles generated by probe sonication was metal particles released by the probe, and to show that particles generated by mixing of ethanol and water were probably oil droplets because they had a density of about 0.8 g/cm^3.

Freeze-thawing

Dispersed particles as well as emulsified oil droplets will be excluded from growing ice and accumulate in the remaining liquid phase, where they will be likely to agglomerate or coalesce. This is likely true also for nanobubbles. In addition, also dissolved gas will accumulate in the liquid phase, leading to nucleation and growth of bubbles. The ability of a dispersion/emulsion to resist freeze-thawing depends on the surface chemistry of the colloids [59], with sterically stabilized colloids being more resistant than electrostatically stabilized colloids [60]. Particle agglomeration may occur even when rapidly freezing a small sample in liquid nitrogen [61]. NTA combined with freezing and thawing of water samples in a regular freezer at −18 °C

has been proposed as a method to detect nanobubbles [62]. Although the authors recognize that nanoparticles may also agglomerate due to freezing, they argue that agglomerated nanoparticles would be detected by NTA, whereas nanobubbles would vanish completely. However, during the several hours of long thawing process, there is plenty of time for particle agglomerates to sediment and for coalesced oil droplets to rise to the surface. Furthermore, large and colloidally unstable agglomerates may also adsorb in the long and narrow capillary through which the water sample is introduced to the NTA measuring cell. This implies that it is unsure whether a reduction in the number of detected particles is due to the vanishing of nanobubbles or due to a loss of particle agglomerates or coalesced oil droplets.

Electron microscopy

Electron microscopy (EM) provides very high resolution and is therefore in principle a powerful tool to detect and characterize nanobubbles. The disadvantage is that these methods are costly, time consuming, and requires much training. In addition, the sample preparation and measurement can potentially affect the sample. Today, there are a multitude of sample preparation and imaging techniques within EM, of which primarily cryogenic methods and liquid transmission electron microscopy (TEM) have been demonstrated for nanobubbles. Furthermore, contrast agent bubbles with thick coatings have been imaged in dry condition [63–65]. EM imaging of nanobubbles in a gel or polymer matrix, is another alternative, which has been demonstrated in the past [35]. Below, cryo-EM and TEM are described in some more detail.

Cryogenic scanning electron microscopy

By freezing water very rapidly, gaseous bubbles can be trapped and subsequently imaged by scanning electron microscopy (SEM) or TEM. Several different sample preparation techniques have been used for imaging of nanobubbles: fracturing of the frozen water so that the bubbles are visible as voids in a flat surface, followed by coating with, e.g., gold before SEM imaging [54], casting of a thin-film replica of the fractured surface and subsequent imaging [66–69] in SEM or TEM, and also direct imaging in TEM of enclosed bubbles [70]. Submicron voids appear to not be a general feature of rapidly frozen water, and the method must therefore be considered valid. However, there are some potential artefact sources that should be discussed. One potential source of artefactual bubbles could be damage from the electron beam, causing bubbling in the ice surface, although such bubbling effects have only been observed in frozen water with a substantial amount of dissolved organic substances [71]. Furthermore, replica casting methods remove this problem, and coating the ice surface with gold also decreases the amount of energy affecting the underlying sample.

Another important issue is how the freezing affects the sample. Extremely fast freezing in, e.g., liquid ethane gives amorphous ice, commonly referred to as vitrified water, whereas freezing in, e.g., liquid nitrogen is slower and usually gives crystalline ice [71]. Dissolved salt as well as solid particles are excluded from crystalline ice and thus tend to accumulate at the freeze-front of growing ice crystals [71]. This is the case also for dissolved gas and slow freezing has been shown to generate macroscopic bubbles [72] at the freeze-front, but how likely this is to occur in cryogenic sample preparation is unclear. In one study, the size distribution of nanobubbles detected in cryo-EM appeared to correlate with the size distribution optically determined by DLS [68]. However, in another study, the sizes of nanobubbles detected by cryo-EM were 5–10 times larger than those optically detected by NTA [54], which the authors concluded were due to bubble coalescence during sample preparation. In several studies, nanobubbles were found also in the control samples, although at lower concentration [67,68]. This finding might be interpreted as bubble formation during the freezing process, and since liquid nitrogen was used in the above referenced studies on uncoated nanobubbles [54,66–69], these results should be treated with some caution. Meanwhile, coated contrast agent nanobubbles [70] as well as uncoated (short-lived) nanobubbles [73] have been imaged directly in TEM following plunge freezing in liquid ethane to form amorphous ice (see Figure 3).

Liquid TEM

EM techniques are most commonly applied to dry samples or frozen liquid samples, as imaging takes place under vacuum. Imaging of liquid samples in TEM has, however, become increasingly popular in recent years [74] because of the availability of more advanced liquid cells for this purpose. As TEM requires very thin samples, the microchip cells used are between 0.1 and 1 μm high and the enclosing windows need to be of extremely thin and strong material. The volume of the cell is only about a nanoliter. The proximity of the cell surface slows down the Brownian motion of dispersed particles considerably and may cause adsorption of colloids. Nevertheless, liquid TEM provides a very interesting possibility to study native dispersions with very high resolution and to differentiate between bubbles, droplets, and particles. The method has been demonstrated for nanobubbles [75] generated in water by a commercial nanobubble generator. However, a prominent feature of this method is that the electron beam supplies much energy to a very small liquid volume, which easily leads to formation of hydrogen bubbles by radiolysis. Electron beam damage to sample cells of graphene has also been shown to lead to bubble formation [76]. This needs to be carefully considered when using the method to detect pre-existing nanobubbles.

Figure 3

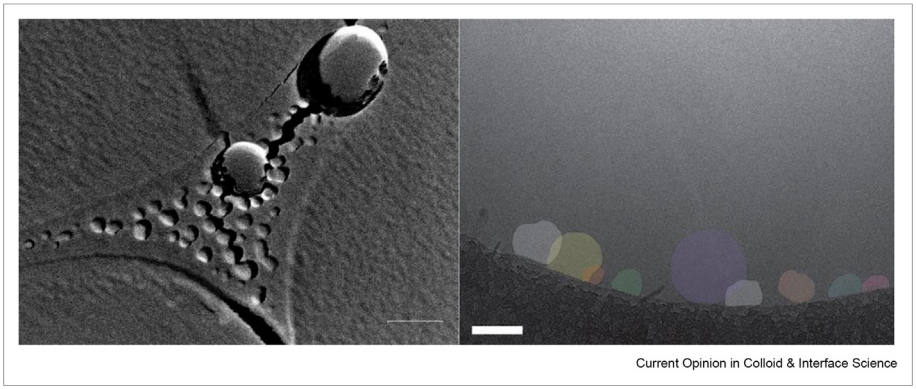

Left: Nanobubbles and impurity particles accumulated at the ice crystallite boundary. Sample frozen in liquid nitrogen, fractured and imaged by thin film replica method. Scale bar 200 nm. Reprinted (cropped) with permission from Uchida, T.; Oshita, S.; Ohmori, M.; Tsuno, T.; Soejima, K.; Shinozaki, S.; Take, Y.; Mitsuda, K., Transmission electron microscopic observations of nanobubbles and their capture of impurities in wastewater. Nanoscale Res Lett 2011, 6 (1), 295 , under the following license: https://creativecommons.org/licenses/by/2.0. Right: TEM image of coated nanobubbles at the surface of the carbon support. Sample frozen in liquid ethane. Bubbles manually colored for better contrast. Scale bar 100 nm. Reprinted (cropped) with permission from Hernandez, C.; Gulati, S.; Fioravanti, G.; Stewart, P. L.; Exner, A. A., Cryo-EM Visualization of Lipid and Polymer-Stabilized Perfluorocarbon Gas Nanobubbles - A Step Towards Nanobubble Mediated Drug Delivery. Sci Rep 2017, 7 (1), 13517, under the following license: https://creativecommons.org/licenses/by/4.0.

Bubble formation can be suppressed by using lower beam intensity [77].

Resonant mass measurement

In resonant mass measurement (RMM), a fine cantilever with an internal channel is used as the sensing unit (Figure 4a). The colloidal particles are passed through the microfluidic channel via two wider bypass channels that are connected to the input and output of the implemented microfluidic channel. The flow though the microchannel is controlled by a pressure difference between the bypass channels. A shift in the resonant frequency occurs as the particles flow through the sensor. The frequency increases if the particles are less dense than the carrier fluid and reduces if the particle density is greater than that of the carrier fluid (see Figure 4b). Thus, the sign of the change in frequency can be used as a tool to distinguish positively buoyant particles from negatively buoyant particles. However, the technique does not directly measure the particle density, as both the density and the particle size contribute to the buoyant mass of the particle. Nevertheless, density determination of colloidal particles using RMM have been reported by several groups [78–80]. In these studies, the density was determined by plotting the buoyant mass versus the fluid density and extrapolating the data to zero buoyant mass. As the density of nanobubbles is expected to be very different from that of nanodroplets and nanoparticles, this method can be adapted to determine the existence and density of nanobubbles. Alheshibri et al. [10,11,49] applied this method to suspected nanobubbles produced by different methods that have been reported to produce long-lived bulk nanobubbles. However, the density of the detected nanoparticles was inconsistent with them being gas-filled nanobubbles, and therefore these results cast doubt on reports of long-lived bulk nanobubbles produced by these methods.

Figure 4

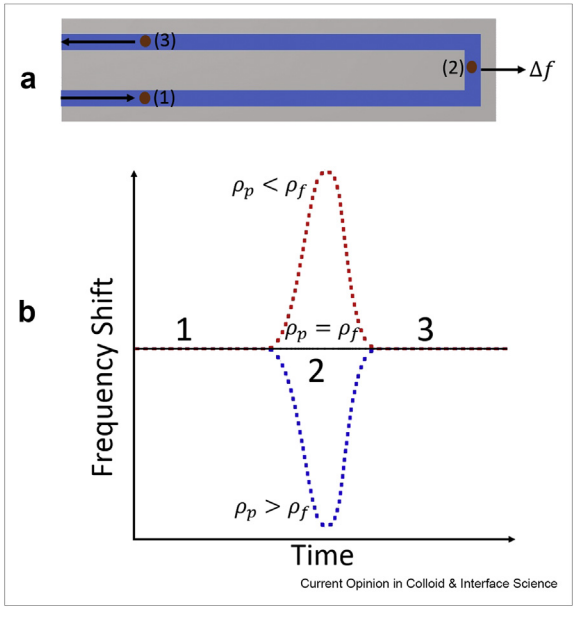

Principle of the resonant mass measurement technique. The technique uses a fine cantilever with an implemented fluidic channel to sense the colloidal particles (panel **a**). The order of movement of the particles as they pass through the channel (1), reach the detecting point (2), and finally exit the channel (3). A shift in the resonance frequency of the cantilever occurs as suspended nanoparticles with density of ($\rho_p \neq \rho_f$) flow through the microchannel, which enables the instrument to distinguish positively buoyant particles ($\rho_p < \rho_f$) from negatively buoyant particles ($\rho_p > \rho_f$) (panel **b**).

Ultrasound response and cavitation

Ultrasound resonance

Owing to the compressibility of gas bubbles, they can be brought into resonance by ultrasound and will therefore scatter ultrasound many orders of magnitude stronger than solid particles of the same size. This effect is used in ultrasound contrast imaging, where coated micro- and nanobubbles are injected to gain contrast. Commonly used ultrasound contrast agents comprise of bubbles in the range 0.5–10 μm. The resonance frequency is inversely proportional to bubble size and is about 1 MHz for a 3 μm bubble [81]. The resonance is also affected by thick and rigid coatings, which may increase the resonance frequency substantially at low sound pressures, but negligibly at >50 kPa. The magnitude of the volumetric oscillations (expansion-contraction) is also affected by the sound pressure, and above 15 kPa also nonlinear and/or nonspherical oscillations will occur, giving a more broadband ultrasound response. Somewhere in the range 200–500 kPa, oscillations are violent enough to cause cavitation and collapse of the bubbles [81]. The resonance weakens with decreasing size, as has been shown both theoretically and experimentally [82] for microscopically visible bubbles in the range 1–4 μm. Nanobubbles are being increasingly explored in ultrasound imaging and for therapeutic purposes, since they are expected to penetrate into tissue where microbubbles cannot reach, but it has been questioned if they can resonate enough at typical imaging frequencies to provide contrast and there is controversy in the field on this issue [3]. Ultrasound contrast from nanobubble preparations have been reported in many papers, but it has been questioned if it is the nanobubbles themselves which provide contrast, or other components in the dispersions. Several novel ultrasound contrast/therapeutic agents comprise other materials than gaseous bubbles [3]. Coated nanodroplets of fluorinated hydrocarbons will be triggered to change to gas phase by ultrasound, something that provides strong contrast. Solid hydrophobic nanoparticles of specific morphologies can act as nuclei for bubble formation, triggered by ultrasound. These are very interesting developments, but points again to the problem with measuring the ultrasound response of a bulk sample—it is not obvious which component in a heterogeneous dispersion, which comprise both particles, vesicles, and bubbles of different sizes, is responsible for the ultrasound response. To address this problem, measurement of single-nanobubble acoustic response have been demonstrated by letting bubbles in a thin focused flow pass an ultrasound transducer [83], although this set-up still does not unambiguously identify which colloidal entities resonate.

Concerning industrial nanobubbles, Leroy et al. [15] used a custom-built ultrasound spectrometer to characterize the output of a commercial nanobubble generator. Based on the measured resonance frequency, it was concluded that only short-lived microbubbles were generated. The method was theoretically expected to be able to detect small nanobubbles at low concentrations, although this was never confirmed experimentally.

Cavitation inception

Cavitation and formation of macroscopic bubbles in liquids takes place due to hydrodynamic conditions, ultrasound, pressure release, and so on. Cavitation normally needs nuclei to occur, free-floating nuclei can be gas bubbles or solid particles [41,84] with gas pockets on their surface. The lower the curvature of the bubble, the lower the subpressure necessary to cause cavitation. At the moderate subpressures, which occur in hydrodynamic cavitation, microbubbles in the range 1–100 μm are probably responsible [22] and their concentration is typically less than 1 per ml [24,25]. Ultrasound can generate higher pressure amplitudes and thus access nuclei of smaller curvature, which can be detected through macroscopic bubbles which form as the ultrasound power is increased. Cavitation inception is thus a useful method to detect gaseous nuclei at very small concentrations, but it is indirect and cannot differentiate between free gas bubbles and gas pockets on solid particles.

Gas detection

Dissolved oxygen

Although other dissolved gases can also be detected in water, quantification of dissolved oxygen (DO) is particularly convenient because of its chemical reactivity. The concentration of oxygen can be determined via Winkler titration or by using an inexpensive digital instrument with a probe of electrochemical or optical type. Measuring the concentration of DO can be used to estimate the degree of air saturation, which is an important parameter in bubble generation. Measurement of DO released by dissolving bubbles can in principle be used to validate the presence of nanobubbles, but as mentioned in the introduction, the volume concentration of air- or oxygen-filled nanobubbles needs to be considerably higher than what is commonly reported for nanobubble preparations, for the released oxygen amount to be detectable. Kikuchi et al. investigated the production of oxygen nanobubbles by electrolysis [85] and detected 30 nm by DLS in the anodic solution. These were reported to be stable for days, although undergoing slow coalescence. DO was measured with a dissolved oxygen meter as well as by Winkler titration. A discrepancy between DO in the native nanobubble dispersion and a 10-fold dilution of the same was assumed to indicate that the nanobubbles released oxygen in the latter case. Lowering the pH, which was expected to destabilize the nanobubbles, also resulted in a higher DO level, which was taken as further

confirmation. Similarly, the same group studied solutions supersaturated with hydrogen gas [86]. They compared the level of hydrogen gas using a dissolved hydrogen meter and a chemical analysis method, the chemical analysis revealed an increase in hydrogen concentration, which was attributed to the presence of hydrogen nanobubbles. In a recent study on biogenic oxygen-filled nanobubbles, it was shown that adding nanobubble solution to N_2-purged solution resulted in several mg/l of oxygen being released [87] as detected by an oxygen probe. In this particular case, the bubble concentration was, however, several orders of magnitude higher than commonly reported for nanobubble preparations, which makes the results credible.

Vibrational spectroscopy

The molecular vibrations of some gases are different depending on if they are in gaseous form or dissolved in water. This can be used to detect bubbles in water. Changes in the rotational fine structure of carbon dioxide was first used to detect surface nanobubbles [88] by infrared spectroscopy and later applied to bulk nanobubbles. Häbich et al. [13] estimated carbon dioxide nanobubbles to be detectable at a concentration of 10^8/ml. Following mixing of ethanol and water, saturated with carbon dioxide to generate bubbles, they detected gaseous carbon dioxide during the first minutes, but concluded it was due to visible larger bubbles and had no correlation with the formed nanoparticles, which remained in dispersion and thus were concluded not to be nanobubbles. However, in another study, infrared spectroscopy was instead used to confirm the presence of CO_2 nanobubbles [89].

Raman spectroscopy has also been used to detect gaseous nanobubbles of nitrogen [66] and methane [90]. Raman spectroscopy can detect the gaseous state of many other molecules [91], such as carbon dioxide and oxygen, which could be useful in bubble research. When a mixture of gases is present (or other molecules in both gaseous and liquid state), the interpretation of vibrational spectra can, however, become ambiguous. Therefore, vibrational spectroscopy is most suitable for chemically simple systems.

Surface charge (zeta potential)

Measuring the mobility of colloids in an electric field enables to find the potential at the slip plane, which is known as the zeta potential [92]. The zeta potential is assumed to be a relatively good measure of the actual surface potential. A high positive or negative zeta potential can prevent colloidal particles, droplets or bubbles from agglomerating or coalescing and is therefore of great practical importance. Colloids can, however, be stabilized by other means, such as steric stabilization by polymer chains, something which is used in coated contrast agent bubbles. As zeta potential has such a great importance for colloidal stability and interaction of nanobubbles with other colloids and surfaces, it has been investigated in many nanobubble studies [9]. A negative zeta potential of high magnitude has even been claimed to be typical of nanobubbles and invoked as evidence that optically detected colloids are nanobubbles [54]. This is further supported by theoretical models for nanobubble stability, which stresses the importance of surface charge [20,21]. However, many different types of colloids have a strong negative zeta potential at neutral or alkaline pH. Adsorption of surface-active material on bubbles may also modify their zeta potential. Furthermore, there has been intense disagreement [93–97] as to whether the clean water–air interface at normal pH has a positive surface charge because of the presence of hydronium ions [95,96] or negative surface charge because of the presence of hydroxide ions [93,94]. This is a challenging problem that has not been solved yet. To conclude, zeta potential is an important property of colloids, but it only provides information about the surface of the colloids, not their interior.

Conclusion

Nanobubbles are being explored for many important applications in medicine as well as industry, but they are also surrounded by controversy. In many cases, solid particles and oil droplets detected by optical methods have probably been mistaken for long-lived nanobubbles, and it can be questioned how common and easily produced long-lived nanobubbles really are. There is therefore a great need for methods that can unambiguously detect nanobubbles in dispersion. In this review, we evaluate a multitude of approaches for the detection of bulk nanobubbles. Methods based on light scattering, such as DLS, NTA, and flow cytometry, do not differentiate between solid particles, liquid oil droplets, or gas bubbles. Light scattering methods can thus not by themselves identify nanobubbles, but may do so in combination with physical perturbation of the sample, such as pressure, vacuum, centrifugation, or ultrasound, which affects bubbles differently than oil droplets and solid particles. Freeze-thawing has also been suggested for such perturbation, but cannot be considered selective enough to only remove bubbles but not particles and droplets. Phase-sensitive optical methods can directly differentiate between positive and negative phase difference relative to water (RI = 1.33) and thus between bubbles (RI = 1.00) and solid particles and oil droplets (RI > 1.33). Holographic particle tracking, using off-axis DHM, can provide quantification of RI and detailed statistical information of dispersions and is thus a powerful method for characterization of nanobubble dispersions.

In addition to optical methods, ultrasound resonance, EM, and RMM can all identify bubbles in dispersion,

although with certain limitations. Ultrasound causes many orders of magnitude stronger resonance in a bubble than a particle of the same size and is a powerful tool to detect bubbles around 1 μm or larger, but there is some controversy around how well it detects bubbles <0.5 μm, which are expected to have a weaker resonance. As an ensemble method, it cannot tell which particular entity in a heterogeneous dispersion causes resonance. EM is a range of methods that are very powerful in terms of size range because of their high resolution, but may affect the sample and create artifactual bubbles in sample preparation as well as during imaging. This needs to be carefully considered when applying such methods to nanobubble dispersions. RMM is meaningful only in combination with a protocol using dilutions in mediums of different density to determine the density of the detected colloids.

Other methods that have been demonstrated concern detection of gaseous molecules in bubbles by vibrational spectroscopy or chemical detection of dissolved oxygen released from nanobubbles. Although these methods are feasible, their sensitivity depends on the volume concentration of nanobubbles and is not sufficient in many cases. Surface charge, measured as zeta potential, is an important property for colloidal stability, but cannot be used to determine if a light scatterer is a bubble or not.

A general conclusion is that combinations of optical detection with other methods, as well as phase-sensitive optical methods based on digital holography, are the most promising routes forward. This is in line with a general trend in particle analysis to move toward automated single-particle characterization and extracting more information about the particles than only hydrodynamic size. This trend is fueled by the availability of better and cheaper optical components and even more by ever improving digital processing capacity. This will greatly benefit research on nanobubbles as well as colloids in general in the years to come.

Declaration of competing interest

The authors declare the following financial interests/personal relationships which may be considered as potential competing interests: Fredrik Eklund is co-founder and CEO of Holtra AB.

Acknowledgements

Muidh Alheshibri acknowledges the funding and support from Deanship of Scientific Research (DSR) at the Imam Abdulrahman Bin Faisal University (IAU), grant No. 2021-065-PYSS.

References

Papers of particular interest, published within the period of review, have been highlighted as:

* of special interest

1. Alheshibri M, Qian J, Jehannin M, Craig VS: **A history of nanobubbles**. *Langmuir* 2016, **32**:11086–11100.

2. Segers T, de Jong N, Lohse D, Versluis M: **Microbubbles for medical applications**. In *Microfluidics for medical applications*. Edited by van den Berg A, Segerink L, London: Royal Society of Chemistry; 2014:81–101.

3. * Stride E, Segers T, Lajoinie G, Cherkaoui S, Bettinger T, Versluis M, Borden M: *Microbubble agents: new directions, ultrasound in medicine & biology*. 2020.
Comprehensive review of the latest developments in ultrasound contrast agents. In addition to gaseous bubbles and their different manufacturing methods, potential therapeutic uses and novel types such as phase change droplets and solid particles are reviewed.

4. Liu Y, Zhou Y, Wang T, Pan J, Zhou B, Muhammad T, Zhou C, Li Y: **Micro-nano bubble water oxygation: synergistically improving irrigation water use efficiency, crop yield and quality**. *J Clean Prod* 2019, **222**:835–843.

5. Ebina K, Shi K, Hirao M, Hashimoto J, Kawato Y, Kaneshiro S, Morimoto T, Koizumi K, Yoshikawa H: **Oxygen and air nanobubble water solution promote the growth of plants, fishes, and mice**. *PloS One* 2013, **8**.

6. Zhu J, An H, Alheshibri M, Liu L, Terpstra PM, Liu G, Craig VS: **Cleaning with bulk nanobubbles**. *Langmuir* 2016, **32**:11203–11211.

7. Haris S, Qiu X, Klammler H, Mohamed MMA: **The use of micro-nano bubbles in groundwater remediation: a comprehensive review**. *Groundw Sustain Develop* 2020, **11**.

8. Shi W, Pan G, Chen Q, Song L, Zhu L, Ji X: **Hypoxia remediation and methane emission manipulation using surface oxygen nanobubbles**. *Environ Sci Technol* 2018, **52**:8712–8717.

9. * Azevedo A, Oliveira H, Rubio J: **Bulk nanobubbles in the mineral and environmental areas: updating research and applications**. *Adv Colloid Interface Sci* 2019, **271**:101992.
Review of industrial nanobubbles and their applications within mineral flotation, water treatment and environmental remediation. Production methods are reviewed and hydrodynamic cavitation is concluded to be most suitable for large scale production.

10. Alheshibri M, Craig VSJ: **Generation of nanoparticles upon mixing ethanol and water; Nanobubbles or Not?** *J Colloid Interface Sci* 2019, **542**:136–143.

11. * Alheshibri M, Craig VSJ: **Differentiating between nanoparticles and nanobubbles by evaluation of the compressibility and density of nanoparticles**. *J Phys Chem C* 2018, **122**:21998–22007.
Suspected nanobubbles, generated by two different commercial nanobubble generators, were found to probably be oil droplets. No significant size change could be seen by DLS when exposed to 10 atm pressure and the density of the particles was determined to be 0.95 g/cm^3 using RMM.

12. * Rak D, Ovadova M, Sedlak M: **(Non)Existence of bulk nanobubbles: the role of ultrasonic cavitation and organic solutes in water**. *J Phys Chem Lett* 2019, **10**:4215–4221.
The density of suspected nanobubbles generated by ethanol–water mixing or probe sonication was inconsistent with them being bubbles. Particle density was estimated by a combination of centrifugation and DLS.

13. Häbich A, Ducker W, Dunstan DE, Zhang X: **Do stable nanobubbles exist in mixtures of organic solvents and water**. *J Phys Chem B* 2010, **114**:6962–6967.

14. * Eklund F, Swenson J: **Stable air nanobubbles in water - the importance of organic contaminants**. *Langmuir* 2018, **34**:11003–11009.
Light scatterers in high concentration salt solutions, previously often assumed to be nanobubbles, were in most cases unaffected by pressure and vacuum and thus probably minerals or other impurities. The effect of contamination on hydrodynamic cavitation experiments was also reported.

15. Leroy V, Strybulevych A, Norisuye T: **Time-resolved ultrasonic spectroscopy for bubbles**. *AIChE J* 2017, **63**:4666–4672.

16. Epstein PS, Plesset MS: **On the stability of gas bubbles in liquid-gas solutions**. *J Chem Phys* 1950, **18**:1505–1509.

17. Duncan PB, Needham D: **Test of the epstein-Plesset model for gas microparticle dissolution in aqueous media: effect of**

surface tension and gas undersaturation in solution. *Langmuir* 2004, **20**:2567–2578.

18. Segers T, Lohse D, Versluis M, Frinking P: **Universal equations for the coalescence probability and long-term size stability of phospholipid-coated monodisperse microbubbles formed by flow focusing**. *Langmuir* 2017, **33**:10329–10339.

19. Yasui K, Tuziuti T, Kanematsu W, Kato K: **Dynamic equilibrium model for a bulk nanobubble and a microbubble partly covered with hydrophobic material**. *Langmuir* 2016, **32**: 11101–11110.

20. Bunkin NF, Shkirin AV, Suyazov NV, Babenko VA, Sychev AA, Penkov NV, Belosludtsev KN, Gudkov SV: **Formation and dynamics of ion-stabilized gas nanobubble phase in the bulk of aqueous NaCl solutions**. *J Phys Chem B* 2016, **120**: 1291–1303.

21. Tan BH, An H, Ohl CD: **How bulk nanobubbles might survive**. *Phys Rev Lett* 2020, **124**:134503.

22. Franc J-P, Michel J-M: *Fundamentals of cavitation*. Kluwer Academic Publishers; 2005.

23. Chang H: **When water does not boil at the boiling point**. *Endeavour* 2007, **31**:7–11.

24. Khoo MT, Venning JA, Pearce BW, Takahashi K, Mori T, Brandner PA: **Natural nuclei population dynamics in cavitation tunnels**. *Exp Fluid* 2020, **61**.

25. Russell PS, Barbaca L, Venning JA, Pearce BW, Brandner PA: **Measurement of nuclei seeding in hydrodynamic test facilities**. *Exp Fluid* 2020, **61**.

26. Elamin K, Swenson J: **Brownian motion of single glycerol molecules in an aqueous solution as studied by dynamic light scattering**. *Phys Rev E* 2015, **91**, 032306.

27. Hassan PA, Rana S, Verma G: **Making sense of Brownian motion: colloid characterization by dynamic light scattering**. *Langmuir* 2015, **31**:3–12.

28. Gross J, Sayle S, Karow AR, Bakowsky U, Garidel P: **Nanoparticle tracking analysis of particle size and concentration detection in suspensions of polymer and protein samples: influence of experimental and data evaluation parameters**. *Eur J Pharm Biopharm* 2016, **104**:30–41.

29. van der Pol E, Coumans FA, Sturk A, Nieuwland R, van Leeuwen TG: **Refractive index determination of nanoparticles in suspension using nanoparticle tracking analysis**. *Nano Lett* 2014, **14**:6195–6201.

30. Block S, Fast BJ, Lundgren A, Zhdanov VP, Hook F: **Two-dimensional flow nanometry of biological nanoparticles for accurate determination of their size and emission intensity**. *Nat Commun* 2016, **7**:12956.

31. Brambila CJ, Lux J, Mattrey RF, Boyd D, Borden MA, de Gracia Lux C: **Bubble inflation using phase-change Perfluorocarbon nanodroplets as a strategy for enhanced ultrasound imaging and therapy**. *Langmuir* 2020, **36**:2954–2965.

32. Jin B, Lin M, Zong Y, Wan M, Xu F, Duan Z, Lu T: **Microbubble embedded with upconversion nanoparticles as a bimodal contrast agent for fluorescence and ultrasound imaging**. *Nanotechnology* 2015, **26**:345601.

33. Shpacovitch V, Hergenröder R: **Optical and surface plasmonic approaches to characterize extracellular vesicles. A review**. *Anal Chim Acta* 2018, **1005**:1–15.

34. Zernike F: **How I discovered phase contrast**. *Science* 1955, **121**:345.

35. Yount D, Gillary E, Hoffman D: **A microscopic investigation of bubble formation nuclei**. *J Acoust Soc Am* 1984, **76**: 1511–1521.

36. Bunkin NF, Shkirin AV, Ignatiev PS, Chaikov LL, Burkhanov IS, Starosvetskij AV: **Nanobubble clusters of dissolved gas in aqueous solutions of electrolyte. I. Experimental proof**. *J Chem Phys* 2012, **137**, 054706.

37. Philips LA, Ruffner DB, Cheong FC, Blusewicz JM, Kasimbeg P, Waisi B, McCutcheon JR, Grier DG: **Holographic characterization of contaminants in water: differentiation of suspended particles in heterogeneous dispersions**. *Water Res* 2017, **122**:431–439.

38. Winters A, Cheong FC, Odete MA, Lumer J, Ruffner DB, Mishra KI, Grier DG, Philips LA: **Quantitative differentiation of protein aggregates from other subvisible particles in viscous mixtures through holographic characterization**. *J Pharmacol Sci* 2020, **109**:2405–2412.

39. * Midtvedt D, Eklund F, Olsén E, Midtvedt B, Swenson J, Höök F: **Size and refractive index determination of Subwavelength particles and air bubbles by holographic nanoparticle tracking analysis**. *Anal Chem* 2020, **92**:1908–1915.
Particle tracking combined with off-axis digital holography was demonstrated for selective detection of surfactant-stabilized nanobubbles in a mixed dispersion. A pressure treatment selectively removed the bubbles, thus confirming the results.

40. Midtvedt B, Olsén E, Eklund F, Höök F, Adiels CB, Volpe G, Midtvedt D: **Fast and accurate nanoparticle characterization using deep-learning-enhanced off-Axis holography**. *ACS Nano* 2021, **14**:2240–2250 (just accepted).

41. Borkent BM, Arora M, Ohl C-D: **Reproducible cavitation activity in water-particle suspensions**. *J Acoust Soc Am* 2007, **121**: 1406–1412.

42. Tuziuti T, Yasui K, Kanematsu W: **Influence of increase in static pressure on bulk nanobubbles**. *Ultrason Sonochem* 2017, **38**: 347–350.

43. Cooke, B. D. J. a. R. C.: **Generation of stabilized microbubbles in seawater**. *Science* 1981, **213**:209–211.

44. Yount DE, Strauss RH: **Bubble formation in gelatin: a model for decompression sickness**. *J Appl Phys* 1976, **47**: 5081–5089.

45. Wang Y, Pan Z, Jiao F, Qin W: **Understanding bubble growth process under decompression and its effects on the flotation phenomena**. *Miner Eng* 2020, **145**.

46. Fang Z, Wang L, Wang X, Zhou L, Wang S, Zou Z, Tai R, Zhang L, Hu J: **Formation and stability of surface/bulk nanobubbles produced by decompression at lower gas concentration**. *J Phys Chem C* 2018, **122**:22418–22423.

47. Olszok V, Rivas-Botero J, Wollmann A, Benker B, Weber AP: **Particle-induced nanobubble generation for material-selective nanoparticle flotation**. *Colloid Surface A* 2020, **592**: 124576.

48. * Alheshibri M, Craig VSJ: **Armoured nanobubbles; ultrasound contrast agents under pressure**. *J Colloid Interface Sci* 2018, **537**:123–131.
Commercial contrast agent bubbles, coated with phospholipids, were exposed to pressure under simultaneous DLS measurement and shown to be compressible. This validated this method to selectively detect nanobubbles.

49. Alheshibri M, Jehannin M, Coleman VA, Craig VSJ: **Does gas supersaturation by a chemical reaction produce bulk nanobubbles?** *J Colloid Interface Sci* 2019, **554**:388–395.

50. Mo C-R, Wang J, Fang Z, Zhou L-M, Zhang L-J, Hu J: **Formation and stability of ultrasonic generated bulk nanobubbles**. *Chin Phys B* 2018, **27**.

51. * Tuziuti T, Yasui K, Kanematsu W: **Influence of addition of degassed water on bulk nanobubbles**. *Ultrason Sonochem* 2018, **43**:272–274.
Nanobubbles produced by a commercial bubble generator were destroyed when the bubble dispersion was mixed with degassed water. This indicates that the detected light scatterers were indeed bubbles.

52. Borden MA: **Lipid-coated nanodrops and microbubbles**. In *Handbook of ultrasonics and sonochemistry*. Edited by Yang G, Zhu J, Okitsu K, Mizukoshi Y, Teo B, Enomoto N, Babu S, Neppolian B, Ashokkumar M, Shaik S, Sonawane S, Singapore: Springer; 2016:1075–1100.

53. Borden MA, Longo ML: **Dissolution behavior of Lipid monolayer-coated, air-filled microbubbles: effect of Lipid hydrophobic chain length**. *Langmuir* 2002, **18**: 9225–9233.

54. * Jadhav AJ, Barigou M: **Bulk nanobubbles or not nanobubbles: that is the question**. *Langmuir* 2020, **36**:1699–1708.
A large number of methods were used to experimentally prove the existence of bulk nanobubbles. Some of the methods are however questioned in this review.

55. Qiu J, Zou Z, Wang S, Wang X, Wang L, Dong Y, Zhao H, Zhang L, Hu J: **Formation and stability of bulk nanobubbles generated by ethanol-water exchange**. *ChemPhysChem* 2017, **18**:1345–1350.

56. Zhou W, Wu C, Lv H, Zhao B, Liu K, Ou L: **Nanobubbles heterogeneous nucleation induced by temperature rise and its influence on minerals flotation**. *Appl Surf Sci* 2020, **508**: 145282.

57. Feshitan JA, Chen CC, Kwan JJ, Borden MA: **Microbubble size isolation by differential centrifugation**. *J Colloid Interface Sci* 2009, **329**:316–324.

58. Supponen O, Upadhyay A, Lum J, Guidi F, Murray T, Vos HJ, Tortoli P, Borden M: **The effect of size range on ultrasound-induced translations in microbubble populations**. *J Acoust Soc Am* 2020, **147**:3236.

59. Wasan DT, Ginn ME, Shah DO: *Surfactants in chemical/process engineering*. M. Dekker; 1988.

60. Kronberg B, Holmberg K, Lindman B: *Surface chemistry of surfactants and polymers*. John Wiley & Sons; 2014.

61. Lepault J, Dubochet J: **Freezing, fracturing, and etching artifacts in particulate suspensions**. *J Ultra Res* 1980, **72**: 223–233.

62. Nirmalkar N, Pacek AW, Barigou M: **On the existence and stability of bulk nanobubbles**. *Langmuir* 2018, **34**: 10964–10973.

63. Tian J, Yang F, Cui H, Zhou Y, Ruan X, Gu N: **A novel approach to making the gas-filled liposome real: based on the interaction of Lipid with free nanobubble within the solution**. *ACS Appl Mater Interfaces* 2015, **7**:26579–26584.

64. Song W, Luo Y, Zhao Y, Liu X, Zhao J, Luo J, Zhang Q, Ran H, Wang Z, Guo D: **Magnetic nanobubbles with potential for targeted drug delivery and trimodal imaging in breast cancer: an in vitro study**. *Nanomedicine* 2017, **12**:991–1009.

65. Batchelor DVB, Abou-Saleh RH, Coletta PL, McLaughlan JR, Peyman SA, Evans SD: **Nested nanobubbles for ultrasound-triggered drug release**. *ACS Appl Mater Interfaces* 2020, **12**: 29085–29093.

66. Ohgaki K, Khanh NQ, Joden Y, Tsuji A, Nakagawa T: **Physicochemical approach to nanobubble solutions**. *Chem Eng Sci* 2010, **65**:1296–1300.

67. Uchida T, Nishikawa H, Sakurai N, Asano M, Noda N: **Ultra-fine bubble distributions in a plant factory observed by transmission electron microscope with a freeze-fracture replica technique**. *Nanomaterials* 2018, **8**:152.

68. Uchida T, Oshita S, Ohmori M, Tsuno T, Soejima K, Shinozaki S, Take Y, Mitsuda K: **Transmission electron microscopic observations of nanobubbles and their capture of impurities in wastewater**. *Nanoscale Res Lett* 2011, **6**:295.

69. * Wang Q, Zhao H, Qi N, Qin Y, Zhang X, Li Y: **Generation and stability of size-adjustable bulk nanobubbles based on periodic pressure change**. *Sci Rep* 2019, **9**.
Bulk nanobubbles were produced in in a clean glass tube by pressure oscillation. In addition to good contamination control, cryo-EM was used to evidence that the bubbles were bubbles.

70. Hernandez C, Gulati S, Fioravanti G, Stewart PL, Exner AA: **Cryo-EM visualization of Lipid and polymer-stabilized Perfluorocarbon gas nanobubbles - a Step towards nanobubble mediated drug delivery**. *Sci Rep* 2017, **7**:13517.

71. Dubochet J, Lepault J, Freeman R, Berriman JA, Homo JC: **Electron microscopy of frozen water and aqueous solutions**. *J Microsc* 1982, **128**:219–237.

72. Lipp G, Körber C, Englich S, Hartmann U, Rau G: **Investigation of the behavior of dissolved gases during freezing**. *Cryobiology* 1987, **24**:489–503.

73. Li M, Tonggu L, Zhan X, Mega TL, Wang L: **Cryo-EM visualization of nanobubbles in aqueous solutions**. *Langmuir* 2016, **32**:11111–11115.

74. Pu S, Gong C, Robertson AW: **Liquid cell transmission electron microscopy and its applications**. *R Soc Open Sci* 2020, **7**: 191204.

75. Sugano K, Miyoshi Y, Inazato S: **Study of ultrafine bubble stabilization by organic material adhesion**. *Jpn J Multiphas Flow* 2017, **31**:299–306.

76. Hirokawa S, Teshima H, Solis-Fernandez P, Ago H, Tomo Y, Li QY, Takahashi K: **Nanoscale bubble dynamics induced by damage of graphene liquid cells**. *ACS Omega* 2020, **5**:11180–11185.

77. Wang L, Liu L, Mohsin A, Wen J, Sheng H, Miller DJ: **Dynamic nanobubbles in graphene liquid cell under electron beam irradiation**. *Microsc Microanal* 2017, **23**:866–867.

78. Patel AR, Lau D, Liu J: **Quantification and characterization of micrometer and submicrometer subvisible particles in protein therapeutics by use of a suspended microchannel resonator**. *Anal Chem* 2012, **84**:6833–6840.

79. Folzer E, Khan TA, Schmidt R, Finkler C, Huwyler J, Mahler H-C, Koulov AV: **Determination of the density of protein particles using a suspended microchannel resonator**. *J Pharmacol Sci* 2015, **104**:4034–4040.

80. Godin M, Bryan AK, Burg TP, Babcock K, Manalis SR: **Measuring the mass, density, and size of particles and cells using a suspended microchannel resonator**. *Appl Phys Lett* 2007, **91**:123121.

81. Roovers S, Segers T, Lajoinie G, Deprez J, Versluis M, De Smedt SC, Lentacker I: **The role of ultrasound-driven microbubble dynamics in drug delivery: from microbubble fundamentals to clinical translation**. *Langmuir* 2019, **35**: 10173–10191.

82. van der Meer SM, Dollet B, Voormolen MM, Chin CT, Bouakaz A, de Jong N, Versluis M, Lohse D: **Microbubble spectroscopy of ultrasound contrast agents**. *J Acoust Soc Am* 2007, **121**: 648–656.

83. Gnyawali V, Wang J-Z, Wang Y, Fishbein G, So LHY, Leon ACD, Abenojar E, Exner AA, Tsai SSH, Kolios MC: *Individual nanobubbles detection using acoustic based flow cytometry*. SPIE; 2019.

84. Bussonniere A, Liu Q, Tsai PA: **Cavitation nuclei regeneration in a water-particle suspension**. *Phys Rev Lett* 2020, **124**, 034501.

85. Kikuchi K, Ioka A, Oku T, Tanaka Y, Saihara Y, Ogumi Z: **Concentration determination of oxygen nanobubbles in electrolyzed water**. *J Colloid Interface Sci* 2009, **329**:306–309.

86. Kikuchi K, Takeda H, Rabolt B, Okaya T, Ogumi Z, Saihara Y, Noguchi H: **Hydrogen particles and supersaturation in alkaline water from an Alkali–Ion–Water electrolyzer**. *J Electroanal Chem* 2001, **506**:22–27.

87. * Song L, Wang G, Hou X, Kala S, Qiu Z, Wong KF, Cao F, Sun L: **Biogenic nanobubbles for effective oxygen delivery and enhanced photodynamic therapy of cancer**. *Acta Biomater* 2020, **108**:313–325.
By using a biologically-derived coating material, a very high concentration of oxygen filled nanobubbles were produced.

88. Zhang XH, Khan A, Ducker WA: **A nanoscale gas state**. *Phys Rev Lett* 2007, **98**:136101.

89. Oh SH, Kim JM: **Generation and stability of bulk nanobubbles**. *Langmuir* 2017, **33**:3818–3823.

90. Uchida T, Yamazaki K, Gohara K: **Generation of micro- and nano-bubbles in water by dissociation of gas hydrates**. *Kor J Chem Eng* 2016, **33**:1749–1755.

91. Tuschel D: **Headspace Raman spectroscopy**. *Spectroscopy* 2014, **29**.

92. Lyklema J: **Interfacial potentials: measuring the immeasurable?** *Substantia* 2017, **1**.

93. Creux P, Lachaise J, Graciaa A, Beattie JK: **Specific cation effects at the hydroxide-charged air/water interface**. *J Phys Chem C* 2007, **111**:3753–3755.

94. Beattie JK, Djerdjev AM, Warr GG: **The surface of neat water is basic**. *Faraday Discuss* 2009, **141**:31–39.

95. Petersen PB, Saykally RJ: **Evidence for an enhanced hydronium concentration at the liquid water surface**. *J Phys Chem B* 2005, **109**:7976–7980.

96. Buch V, Milet A, Vácha R, Jungwirth P, Devlin JP: **Water surface is acidic**. *Proc Natl Acad Sci Unit States Am* 2007, **104**:7342–7347.

97. Sengupta S, Moberg DR, Paesani F, Tyrode E: **Neat water–vapor interface: proton continuum and the nonresonant background**. *J Phys Chem Lett* 2018, **9**:6744–6749.